RSC Advances

ROYAL SOCIETY OF CHEMISTRY

www.rsc.org/advances

Graphical Abstract:

Growth kinetics of membrane stabilized silver nanoparticles has been studied for the first time with time resolved in-situ SAXS. Also the catalytic application of thus formed nanocomposite membranes has been explored.

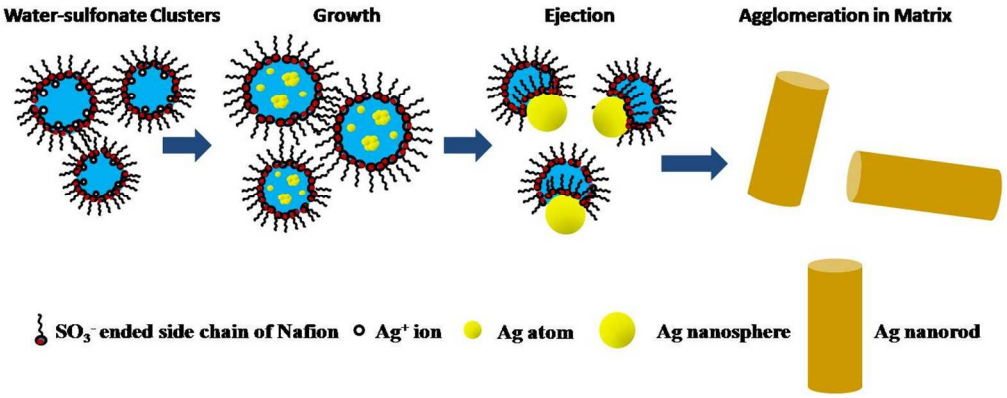

Cite this: DOI: 10.1039/c0xx00000x

www.rsc.org/xxxxxx

PAPER

Time Resolved Growth of Membrane Stabilized Silver Nanoparticles and their Catalytic Activity

Sabyasachi Patra,[a] Debasis Sen,[b] Ashok K. Pandey,[a] J. Bahadur, [b] S. Mazumder, [b] Shobha V. Ramagiri,[c] Jayesh R. Bellare,[c] S. V. Roth,[d] G. Santoro, [d] S. Yu, [d] A. Goswami*[a]

Received (in XXX, XXX) Xth XXXXXXXXX 20XX, Accepted Xth XXXXXXXXX 20XX
DOI: 10.1039/b000000x

Formation of highly stable metal nanostructures in Nafion® membrane with various aspect ratios has been of considerable research interest in recent years. However, there is a need for a proper understanding of the growth mechanism of such nanostructures in Nafion® (sometimes larger than the size of water-sulfonate ionic clusters of the membrane). In this work, we reveal for the first time the early growth kinetics of silver nanoparticles in Nafion®-117 ion-exchange membrane during in situ L-ascorbic acid reduction of Ag^+ ions by time resolved in situ small-angle X-ray scattering (SAXS) using synchrotron radiation with a time resolution of 50 ms. The SAXS analyses, corroborated by transmission electron microscopy (TEM), showed that the sizes of nanoparticles increase rapidly along with their number density until they attain certain size that could be accommodated in the ~5 nm water-sulfonate ionic clusters. Further growth takes place either by self-agglomeration of the particles ejected out from the water-sulfonic acid clusters or by continuous reduction of metal ions on the existing nanoparticle surfaces (uniformly or at some specific facet) leading to formation of bigger nanostructures with various aspect ratios. The time resolved information of nanoparticles growth provides an opportunity for the controlled synthesis of metal nanoparticles with a definite size, shape and size distribution for a specific application. The catalytic properties of Ag nanoparticles formed in the membrane were examined using borohydride reduction of a model dye methylene blue (MB). It was observed that smaller Ag nps with a mean diameter ~ 3 nm those confined in the hydrophilic clusters of the Nafion® matrix, have reasonable good catalytic activity and lower lag time for onset of reduction.

INTRODUCTION

Metal nanoparticles (nps) assembly offers numerous technological possibilities.[1] Therefore, recent emphasis of materials engineering is focused on development of advanced functional materials in which atleast one of the components presents dimensions in the nanometer range. Metal nanoparticles embedded in synthetic polymer membranes are being developed for a variety of advance applications such as water purification, catalytic applications, chemical sensors, actuators, fuel cell, water splitting, sequestering of ions, substrates for surface enhanced Raman scattering etc.[2] The physical architecture and chemical composition of the membrane as well as shape, size and spatial distribution of the nanoparticles play an important role in the success of the nanocomposite membrane designed for a specific application. Understanding the growth mechanism that governs the size, shape and spatial distribution of the nanoparticles is therefore crucial to prepare tailor-made membrane nanoparticles composite for a given application.

The most extensively used membrane for hosting a variety of nanoparticles is poly(perfluorosulfonic) acid (Nafion®-117) ionomer membrane.[3] The chemical structure of Nafion®-117 consists of poly(tetrafluoroethylene) (PTFE) domains that maintain the structural integrity and provide superior chemical and thermal stability.[4] The sulfonic acid groups, attached to randomly spaced long perfluorovinyl ether chains form nanosized water-sulfonic acid clusters with diameters around 5 nm. Nafion® is a non-porous membrane but presents a microstructure when being hydrated. The microstructure of Nafion® consists of three regions, the hydrophobic fluorocarbon backbone, hydrophilic sulfonic acid clusters, and an interfacial region.[4] Several models have been suggested for the physical structure of water swollen Nafion®.[5] The most recently accepted morphological model suggested a bi-continuous network of the water-sulfonic acid clusters embedded in a matrix of PTFE.[6]

The formation of metal nanoparticles in Nafion® membrane involves loading of desired precursor metal ions by ion-exchange and subsequent in-situ reduction with a suitable reducing agent. It has been observed by transmission electron microscopy (TEM) that the size, shape and spatial distribution of the nanoparticles are strongly influenced by the nature of the reducing agent, extent of precursor ions occupying ion-exchange sites, temperature during the reduction and the time of reduction.[7] Though

literatures exist on growth kinetics of nanoparticles in aqueous solution, there are limited studies on the topic in nanoconfined media where both nanoconfinement and restricted diffusion of reactant can significantly affect the growth process. It is most likely that the initial growth of metal nanoparticles occurs in the nanoconfined hydrophilic sulfonate clusters in Nafion®. This is because of the fact that water soluble reductant and metal precursor ions access the membrane matrix through channels formed by inter-connected network of hydrophilic ionic clusters. However the formation of metal nanoparticles with different sizes and various aspect ratios in such ~5 nm hydrophilic templates is not well understood. There are scarcely studies on the time dependent growth of nanoparticles in a Nafion® matrix due to the inherent difficulty involved in such study. TEM in combination with time resolved SAXS can provide valuable information of the nanoparticle growth mechanism.

Here, in order to investigate the mechanism behind the formation of metal nanoparticles, the early growth kinetics of silver nanoparticles by ascorbic acid reduction in Nafion®-117 membrane has been studied by time resolved in situ SAXS using synchrotron radiation with a time resolution of 50 ms. Ascorbic acid has been chosen because of its interesting role as a weak reductant for growth of metal nanoparticles with various aspect ratios.[8] A plausible mechanism for Ag nanoparticles growth confined in the water clusters has been elucidated. The time resolved information of nanoparticles growth obtained in the present work holds promise for controlled synthesis of silver nanoparticles in Nafion® membrane with tunable size, shape and spatial distribution. In addition, the redox catalytic activities of spherical Ag nanoparticles stabilized in the hydrophilic clusters (particles with size less than 5 nm) and of bigger nanorods stabilized in soft PTFE matrix (nanostructures with sizes bigger than the size of ionic clusters) have been studied for catalytic bororhydride reduction of methylene blue.

EXPERIMENTAL SECTION

Materials and Methods. Nafion®-117 ionomer membrane with an equivalent weight of 1100 g/SO_3H was purchased from Ion Power Inc. Analytical reagent grade chemicals $AgNO_3$, $NaNO_3$ and ascorbic acid were purchased from BDH (Poole, England). De-ionised (DI) water (18 MΩ cm^{-1}) was used throughout the experiment for preparing solutions. Nafion®-117 membrane was pre-conditioned by following standard treatments as described elsewhere,[9] and cut into 2×2 cm^2 piece. Ag^+ ions were loaded in the matrix by equilibrating into 0.5 mol L^{-1} $AgNO_3$ solution for 30 min with continuous stirring. The fully Ag^+ loaded ionomer samples were equilibrated with well-stirred 0.25 mol L^{-1} $NaNO_3$ solution for 30 s to prepare a sample having 25 % Ag^+ loading. The time required for preparing sample having the desired load of Ag^+ ions was fixed based on previous studies.[10] Fully Ag^+ loaded samples were not considered for this study to avoid any possibility of metallization due to a high silver content.

Nanoparticle synthesis. Two small pieces of Nafion® films (2×2 cm^2) of which 25 % of the ion-exchange sites are loaded with Ag^+ ions were reduced with 0.1 mol L^{-1} ascorbic acid solution at room temperature for 1 min and 5 min[7c] respectively. Thin metallization of silver appeared on the membrane surface, which could easily been removed by soft rubbing with wet tissue paper. The prepared samples were then subjected to TEM characterization.

TEM Characterization. Transmission electron microscopy (TEM) was carried out on cross-sections of the prepared nanocomposite membrane samples. Prior to microscopy, the samples were equilibrated with 0.25 mol L^{-1} $NaNO_3$ solution to ensure the removal of any unreduced Ag^+ ions. The nanocomposite films were sectioned under cryogenic environment in a Leica ultramicrotome to 70 nm thickness. The sections were collected on 200 mesh formvar and carbon coated Cu grids. The grids were examined in an FEI Technai G2 electron microscope at IIT Bombay, at 120 keV without any external treatment.

In-situ time resolved SAXS Study by Synchrotron Radiation. The SAXS experiments were carried out at the P03/MiNaXS beamline at PETRA-III, DESY, Hamburg, Germany.[11] The wavelength of incident micro-focused X-ray beam was 0.957 Å and the beam size was 32 μm (H) × 23 μm (V). A 2-dimensional Pilatus 300K (Dectris Ltd., Switzerland) detector was used to acquire the scattering patterns. The sample to detector distance was 3.3 meter. A flow reactor cell made of Perspex® equipped with Kapton® windows was used as a sample holder. Nafion®-117 matrix (2×2 cm^2), preconditioned and loaded with Ag^+ ions (25 % Ag^+ loading) was placed in the sample holder containing a small opening for the injection of reducing solution (ascorbic acid). Ascorbic acid (0.1 mol L^{-1}) solution was fed through an injection syringe with a rate of 0.2 mL / 5 s to sample holder ensuring the alignment of ascorbic acid drops to the beam. A schematic of the experimental setup is shown in Figure 1. The reaction started at room temperature. A maximum time resolution of 50 ms has been achieved with reasonable statistics in the scattering profiles. Ten consecutive profiles were averaged for further analysis to improve the statistics of the scattering data.

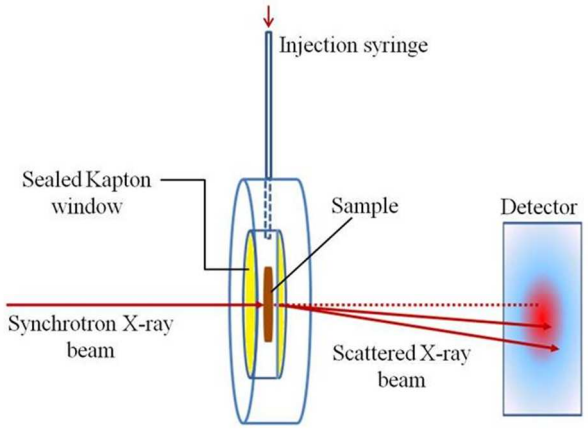

Figure 1. Schematic diagram of the experimental setup for in situ SAXS experiment.

Catalytic reduction of methylene blue. Room temperature borohydride (BH_4^-) reduction of a model dye methylene blue (MB) was studied using the Ag nanoparticles embedded Nafion®-117 membranes as solid phase catalyst. The two nanocomposite film samples used were prepared by ascorbic acid reduction for 1 min and 5 min as described above. To continuously monitor the reaction spectrophotometrically, the reduction was carried out in a quartz cell with a path length of 1 cm. Typically, the

composition of reaction solution was 100 µL of 0.2 mmol L^{-1} MB + 1800 µL water + 200 µL 0.2 mol L^{-1} of freshly prepared $NaBH_4$. A piece ($1 \times 2\ cm^2$) of membrane/Ag nanoparticles composite was inserted without obstructing light path in the solution filled quartz cell placed in a portable UV-VIS spectrophotometer (K-MAC, South Korea). The UV-VIS absorption spectra were recorded with a fixed time interval (30 sec or 1 min) in the scanning range of 200-700 nm at room temperature (25 °C). While recording the spectra the spectrophotometer was placed on a magnetic stirrer. A small magnetic bar was inserted in the quartz cell for continuous stirring of the reaction solution without disturbing the absorbance measurement. The stirring rate was fixed at 300 rpm. The progress of the reaction was monitored at absorbance 665 nm (λ_{max} for MB). After the completion of the reaction the membrane was removed from the reaction mixture, washed with water, and dried at room temperature for its use in the next cycle.

THEORETICAL SECTION

SAXS analysis: The scattering patterns, recorded on a two-dimensional Pilatus detector (Pilatus 300K), have been converted to one-dimensional scattering profiles to obtain the scattering vector (q) dependence of the scattering intensities by azimuthal integration. The scattering contribution of the pristine ionomer matrix (Ag^+ loaded) has been subtracted from each scattering curve of the ascorbic acid treated Nafion® (silver nanoparticles embedded). The size dispersion of the formed silver nanoparticles has been analysed based on non-linear least square fitting of the recorded scattering curve considering polydisperse spherical particle model which is supported by transmission electron microscopy. For such a case, the scattering intensity I(q) may be approximated as,

$$I_1(q) = I_{NS}(q) = \left(\int_0^\infty P_{NS}(q,R) R^6 D_{NS}(R) dR \right) \quad (1)$$

where, $P_{NS}(q,R)$ represents the form factor of a nanostructure. $D_{NS}(R)$ represents the nanostructure size distribution and R the particle radius. For spherical nanostructures of radius R, the form factor is analytically solvable presenting the following expression.

$$P_{NS}(q,R) = 9 \frac{(\sin(qR) - qR\cos(qR))^2}{(qR)^6} \quad (2)$$

In the present case, standard lognormal distribution of following type

$$D_{NS}(R) = \frac{1}{\sqrt{2\pi\sigma^2 R^2}} \exp\left[-\frac{[\ln(R/R_0)^2]}{2\sigma^2} \right] \quad (3)$$

was considered for the size distribution, where R_0 represents the median radius and σ represents the polydispersity index of the distribution.

RESULTS AND DISCUSSION

L-ascorbic acid is a highly polar compound with very high solubility in water. It behaves as a vinylogous carboxylic acid with involvement of the lone pair on the hydroxyl group, the ring double bond, and the carbonyl double bond acting as a conjugated system. The hydroxyl proton situated at the end of the vinyl group is extraordinarily acidic compared to a common alcohol hydroxyl group because of the extra stability of the conjugate base of ascorbic acid by two major resonance structures.

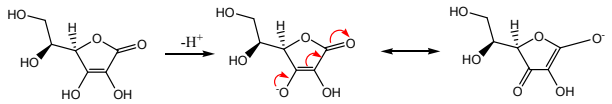

Scheme 1. Resonance structures in conjugate base of L-ascorbic acid.

The pH of the L-ascorbic acid solution used in the present study was 2.63. At this low pH, ascorbic acid is expected to be present as neutral molecule (AH_2) and a small fraction will be present as ascorbate anion (AH^-) ($pK_a = 4.26$). The ascorbate anion (AH^-) is mainly responsible for the silver ions reduction in the membrane as it is more reactive than ascorbic acid (AH_2) in electron transfer reaction.[12] The chemical reduction of Ag^+ ions by ascorbic acid follows first order kinetics on ascorbic acid and silver ion concentrations, together with an inverse first-order dependence on H^+ ions concentration.[13] The reaction involves the transfer of two electrons and the formation of dehydroascorbic acid (A).[13] S.P. Mushran et al. have monitored the progress of the reaction between ascorbic acid and silver ions and have demonstrated the stoichiometric equation for the reduction of silver ions with ascorbic acid (AH_2) as shown in scheme 2.[13] The mechanism involves the interaction of Ag^+ ions with the ascorbate anions (AH^-), which is the slowest step, resulting in the formation of a free radical ($AH^\cdot$), attacked by a second silver ion to form dehydroascorbic acid (A).[13] Because of the proton release, the reduction potential of the system is pH dependent.

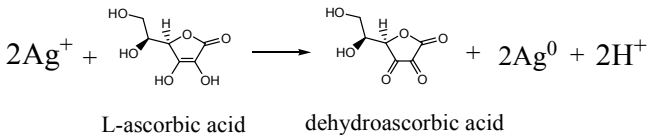

Scheme 2. Stoichiometric equation for the reduction of silver ions by L-ascorbic acid.

Time resolved SAXS using synchrotron radiation is well suited to follow the in-situ nps formation (number density) and their growth kinetics (size) with millisecond time resolution. The utility of synchrotron radiation-based X-ray reflection and scattering techniques in dimensional nanometrology is recently reviewed by Krumrey et al.[14] In present work, the in situ formation of Ag nps in Nafion®-117 during L-ascorbic acid reduction was studied by time resolved in situ SAXS using synchrotron radiation. The temporal evolution of radial averaged SAXS profiles and corresponding increase in median nps diameter as a function of time are shown in Figure 2. In Figure

2a, it is seen that the SAXS patterns evolved continuously with time revealing the in-situ growth of Ag nps. However, the median diameter observed form the SAXS profile at the earliest time is 2.6 nm as shown in Figure 2b. The particles are likely to be formed by means of monomer addition after a discrete nucleation period. Takesue et al. have shown that in aqueous medium the first full-shell clusters Ag_{13} (size 0.7 nm) were involved in growth of Ag nps.[15] They could observed the Ag_{13} clusters with time resolution of 0.18 ms in their in situ experiment. Hence, the nucleation and initial growth may be too fast to be observed with the achieved time resolution of the present work. Though the very early stages could not be resolved, the present study is the first of its kind showing that the evolution of nanoparticle size in a nanoconfined medium (polymer membrane) is an inherently much slower process than the one observed in bulk solution.

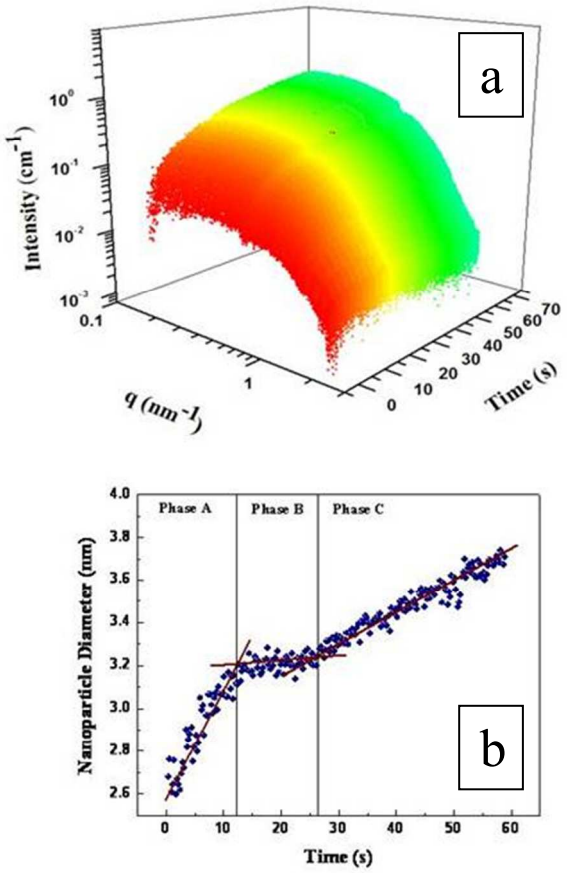

Figure 2. In-situ time resolved SAXS profiles of during Ag nps formation and growth during ascorbic acid reduction in Nafion® (a), and corresponding evolution of median diameter of Ag nps (b) as a function of reduction time.

It has been previously reported that the process of nucleation and growth of the Ag nps in aqueous medium was completed in very short reaction time of ca. 6 ms.[15] In Figure 2b it is clearly shown that the growth of the Ag nps continued for a longer period of time, revealing that the growth mechanism inside the nanodomains of a Nafion® membrane is different from that of bulk. The growth profile of Ag nps could be divided into three distinct phases as shown in Figure 2b. The phase A showed a fast growth of Ag nps as evidenced by higher slope up to ~3.2 nm. The rate of the Ag nps growth reached a plateau in about 12 s (Phase B). The further growth was noticed after a lag time of about 14 s, and thereafter progressed with slower rate (Phase C).

Mechanism of growth: The particles size distributions as a function of reduction time as obtained from analysis of SAXS data are shown in Figure 3. The initial particle size distribution curve is almost symmetric ranging from 1.2 nm to 5 nm (standard deviation = 0.63). The particles with such size distribution profile could be accommodated in the water-sulfonate clusters of the membrane. As time progressed, the size distribution curves broaden and became more asymmetric i.e. left side remained at 1.2 nm but right side of the curve shifted systematically from 5 nm to 8 nm (standard deviation = 1.13). This is possible only when there was continuous birth of new particles to compensate for the particles undergoing growth (shifted to right side). It is interesting to note that all the particle size distribution curves start from 1.2 nm that is size of second full-shell Ag_{55} cluster.[16] After 10 s, the particle size distribution curve stretches beyond 5 nm sizes that cannot be accommodated in the ~5 nm water-sulfonate clusters and must have started ejecting from them. The ejection of nanoparticles from the ionic clusters has been corroborated by the existence of the ionomer peak at higher scattering vector (q) regime in the SAXS profiles of Ag nps embedded Nafion®-117.[7c] The median diameter increased slowly from 2.6 to 3.2 nm. Thereafter, the increase Ag nps diameter became considerably slower.

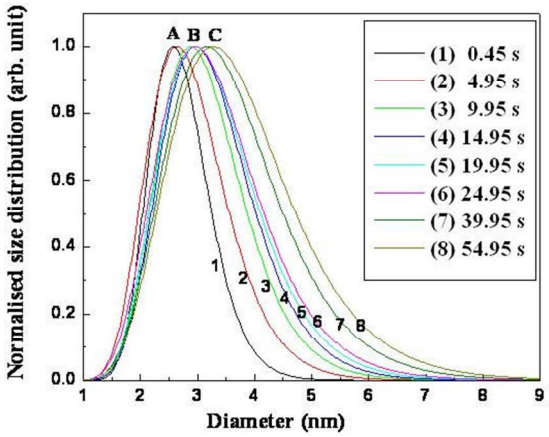

Figure 3. Temporal evolution of Ag nps size distributions deduced from SAXS profiles.

To understand how the continuous supply of monomer and birth affects the number density, a variation of the number density (particles cm^{-3}) of Ag nps during the reduction process was deduced from the time resolved SAXS profiles. It is seen in Figure 4 that the particle number density increased continuously till ~ 25 s. This suggests that the birth of new particles was sustained even in the phase B (see Figure 2b) where median diameter growth showed a lag time. In addition, there is a change in the slope of the particle number density at 2-3 s indicating slowing down of the birth rate of new particles. Initial fast birth rate could be attributed to ascorbic acid reduction at the surface layer of the membrane. After 25 s, the number density profile decreased slowly in phase C indicating a significant decrease in

the birth rate and onset of agglomeration of bigger Ag nps ejected to the adjoining PTFE matrix.

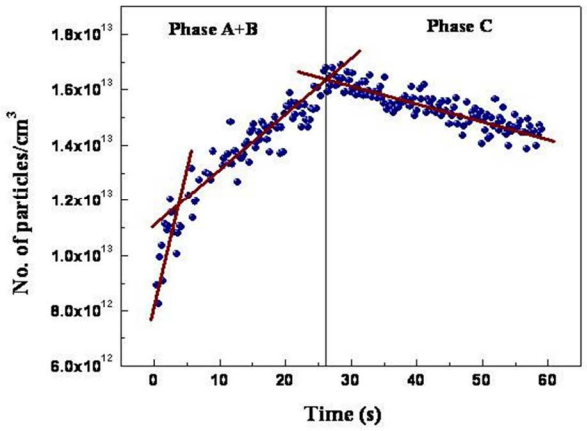

Figure 4. Time dependence of the number density (particles cm^{-3}) of Ag nps during in situ reduction.

TEM analysis of samples prepared in the same conditions was carried out. Figure 5 presents the TEM image of the membrane crossection after reduction for 60 s and the respective size distribution histogram. Formation of uniformly distributed ~3 nm silver nanoparticles is observed. The results obtained in the SAXS experiment (Figure 3) are in reasonably good agreement with TEM analysis (Figure 5).

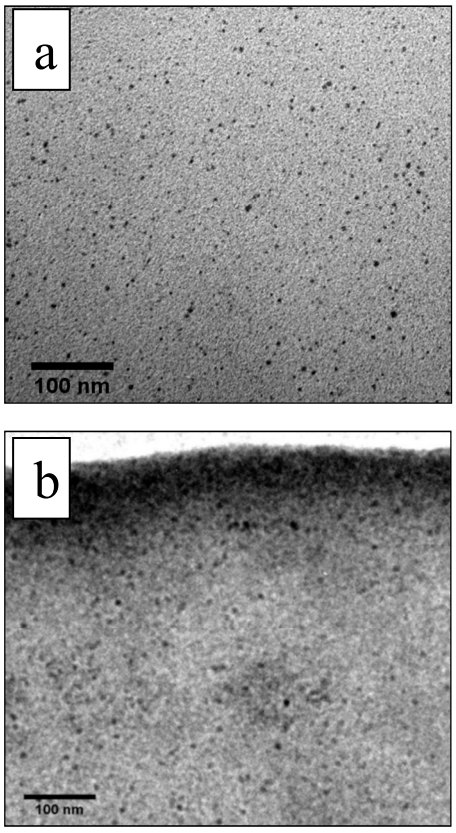

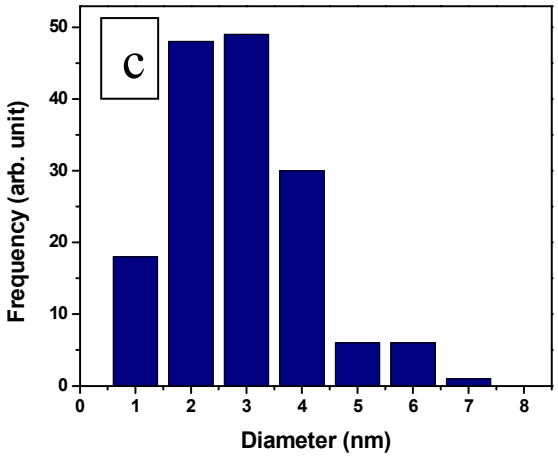

Figure 5. TEM image of cross section of Nafion® sample subjected to reduction with ascorbic acid for 60 s (a,b) and size distribution histogram of Ag nps as obtained from the TEM images analysis (c).

The nanoparticles produced at 60 s of chemical reduction possess significant size dispersion with mean diameter of ~3 nm. The wider size distribution of nanoparticles in SAXS analysis data in comparison to TEM analysis data can be attributed to the contribution of bigger particles formed on the matrix surface to the size distribution profiles extracted from the SAXS experiments, as the characterization based on scattering technique probe larger fraction (both interior and surface) of the samples. The mean diameter value and the low degree of polydispersity of the formed nanoparticles exactly mimicking the water-sulfonate clusters (3-5 nm) in Nafion®-117, provide clear evidences for the existence of such hydrophilic clusters in Nafion® and their templating activity.

It was observed in our previous work that extending the reduction time upto 5 min under similar experimental conditions led to the formation of nanorods.[7c] In order to study the spatial distribution of such nanostructures, the TEM images across the thickness of membrane were studied. Figure 6 presents the TEM image of a sample after 5 min of reduction, showing the formation of uniformly distributed nanorods (~8 nm diameter and ~40 nm length) across the membrane thickness. It is clear from the Figure 5a and 6 that, the particle number density (number of particles per unit area of the membrane) decreases significantly from 1 min (Figure 5a) to 5 min (Figure 6) of reduction process. This fact suggests that the smaller ~3 nm particles formed at 1 min of reduction are the building block units for the formation of bigger nanorods (~40 nm length) by sacrificial self-agglomeration in a preferential direction leading to the formation of 1-D nanostructures (nanorods) in the surrounding PTFE matrix.

Redox Catalytic Activity of Ag Nanoparticles in Nafion®-117 Matrix. The redox catalytic activities of Ag nanoparticles formed by the reduction of Ag^+-loaded Nafion®-117 by ascorbic acid for 1 min (nanosphere) and 5 min (nanorods) were studied at room temperature for borohydride reduction of a model dye methylene blue (MB). The choice of these two Ag-Nafion® samples was based on the fact that ~3 nm spherical Ag nps are formed after 1 min as described above, and 5 min reduction lead to a formation of bigger nanostructures with sizes larger than 10 nm (spherical

or rod) as shown in Figure 7.

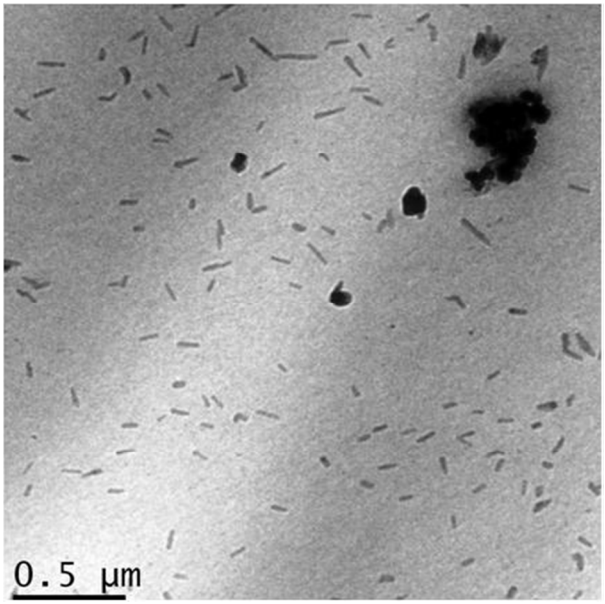

Figure 6. TEM images showing spatial distribution of Ag nanorods across thickness of the membrane subjected to reduction with ascorbic acid for 5 min.

There are two factors that may be responsible for the catalytic activity of the Ag nanoparticles, the size/shape of the particles and their accessibility to reactants MB and BH_4^- ions. The Ag nanoparticles mediate electron transfer after chemisorptions of MB and BH_4^- on its surface. Figure 7a gives the representative time resolved UV-VIS absorption spectrum of MB undergoing catalytic reduction in presence of the Ag nanosphere embedded catalyst membrane. The gradual decrease of the peak intensity at 665 nm with time shows the decrease in MB concentration in bulk solution. This may be due to two modes: the sorption of MB by the membrane, which is a diffusive process and the catalytic reduction of MB. The curve (iii) in Fig. 7b represents the rate of decrease of MB concentration in the solution due to its diffusion into the Ag nanosphere loaded membrane in absence of BH_4^-. Curve (i) and (ii) represents the rate of decrease of MB concentration in presence of the reducing agent (BH_4^-) for the sample with Ag nanospheres and Ag nanorods respectively. In both the cases, initially the curves are exactly superimposed on the curve (iii) indicating absence of catalytic reduction of MB during the period (lag phase). The decrease in MB concentration during this lag phase is therefore attributed to the diffusion of MB into the membrane. However, beyond the lag phase the catalytic reduction of MB is a parallel process, resulting in a increased slope of the curves. The catalytic reduction of MB with BH_4^- follows pseudo-first-order kinetics described by:

$$\ln(A_t/A_0) = - kt \quad (4)$$

where A_0 and A_t are the initial absorbance and at time t, respectively, and k is the catalytic reduction rate constant.

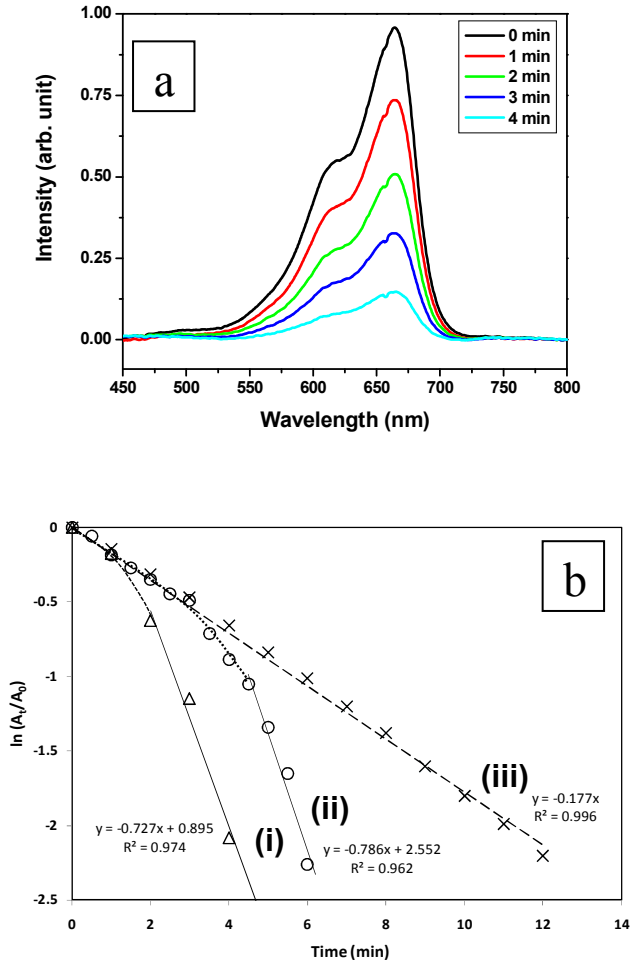

Figure 7. (a) Successive UV−vis spectra of catalytic reduction of MB by $NaBH_4$ in the presence of Ag nanosphere embedded Nafion®-117 membrane (1 min reduction), and (b) Variation of logarithm of A_t/A_0 as a function of reduction time in the presence of Ag nps loaded membrane samples formed by ascorbic acid reduction for 1 min (Δ) and 5 min (O). The dashed line plot (X) shows the variation of A_t/A_0 with time in absence of the reducing agents (only because of diffusion of MB through Ag nps (1 min) embedded Nafion®). A_t and A_0 represent absorbance of 665 nm at time t and initial time, respectively.

The occurrence of a lag phase in the metal nanoparticles catalyzed redox reaction has been observed by many researchers.[17] A possible explanation has been given by Ray et al. in terms of passivation of metal nanoparticles in aqueous environment, which reduces their catalytic activity.[18] On addition of BH_4^-, the nanoparticles are depassivated, restoring their catalytic activity. The lag time has been attributed to the depassivation phase, when no reduction occurs. After the lag time, the catalytic reduction of MB occurs, increasing the rate of disappearance of MB concentration in the bulk solution. They have shown that, with increase in the catalyst concentration, such lag phase is reduced. In the present work, both the effect of passivation as discussed by Ray et al and the diffusion of reactants (both MB and BH_4^-) into the membrane considerably influences the reaction kinetics. Nafion®-117 membrane consists of fixed anionic charge sites, and it will expel the negatively charged BH_4^- ions by Donnan exclusion. So the catalytic reduction is expected to occur largely on the membrane surface. Since the metal particles on the membrane surface are exposed to

atmosphere, their surfaces will be passivated which leads to the appearance of an lag phase. In presence of borohydride, the catalytic activity of the nanoparticles is slowly restored, and the reduction of MB on the membrane surface starts, which leads to the rapid increase in the slope of ln (A_t/A_0) vs. t plot. For curve (i) and (ii), the values of k from the slopes of linear portion of curves are found to be nearly same (0.727 min^{-1} and 0.786 min^{-1} respectively), indicating same rate of reduction. This is probably due to reduction occurring at the surface of the membrane under identical chemical environment making the rate constants similar. The difference in lag time may be due to difference in depassivation time in the two samples which may be due to difference in surface number density/morphology of the nanoparticles in the two samples.

CONCLUSIONS

In the present work it has been demonstrated that early growth of spherical Ag nanoparticles in size of ~ 3nm takes place in the water-sulfonate clusters of Nafion®-117 matrix by room temperature ascorbic acid reduction. The whole process can be divided to three stages: a rapid initial formation and growth followed by, a saturation of the nps size with continuous increase in number density, and a further slow increase in nps size and decrease in number density. Further growth by sacrificial self-agglomeration takes place after ejection of nanoparticles from water-sulfonate clusters leading to formation of rod-like shaped nanostructures with bigger sizes. This study demonstrated the possibility for controlled synthesis of Ag nps in Nafion® membranes with different shapes and sizes. The analytical tool employed in the present work can also be used for the study of growth mechanism of other metal nanoparticle (Au, Pt, Pd etc.). The Ag nanoparticles confined in the membrane water-sulfonate clusters or ejected to the PTFE matrix show good redox catalytic activity. A higher lag time in the onset of reduction was observed for the samples with larger Ag nanostructures in comparison to those confined in water clusters transport channels. This has been attributed to the difference in surface number density/morphology of the nanoparticles in the two samples.

Acknowledgements. DS and JB thankfully acknowledge the Department of Science and Technology (DST), India for providing financial support (1-20110533) for the experiment at PETRA-III, through Saha Institute of Nuclear Physics (SINP), Kolkata, India. This work was carried out at the P03 beamline of the light source PETRA III at DESY. DESY is a member of the Helmholtz Association (HGF). S.Y. acknowledges the kind financial support for Knut och Alice foundation. The authors thank the CryoTEM Facility of IIT Bombay for TEM access.

Notes and references

[a]*Radiochemistry Division,and* [b]*Solid State Physics Division, Bhabha Atomic Research Centre, Mumbai-400 085, India*
[c]*Department of Chemical Engineering, I.I.T. Bombay, Powai, Mumbai 400 076, India*
[d]*Deutsches Elektronen-Synchrotron (DESY), Notkestr. 85, D-22607, Hamburg, Germany*
**Corresponding author: FAX: +91-22-25505150/25505151, Tel: +91-22-25593688 E-mail: agoswami@barc.gov.in*
See DOI: 10.1039/b000000x/

(1) (a) S. Kinge, M. Crego-Calama, D.N. Reinhoudt, *ChemPhysChem* **2008**, *9*, 20-42. (b) A.N. Shipway, E. Katz, I. Willner, *ChemPhysChem* **2000**, *1*, 18-52. (c) O.R. Bolduc, J.-F. Masson, *Anal. Chem.* **2011**, *83*, 8057-8062. (d) Y. Shen, L. Zhao, L. Qi, J. Qiao, L. Mao, Y. Chen, *Chem. Eur. J.* **2012**, *18*, 13755-13761. (e) Y. Ofir, B. Samanta, V.M. Rotello, *Chem. Soc. Rev.* **2008**, *37*, 1814-1825.

(2) (a) V.V. Volkov, T.A. Kravchenko, V.I. Roldughin, *Russ. Chem. Rev.* **2013**, *82*, 465-482. (b) G. Zhu, Y. Liu, Z. Xu, T. Jiang, C. Zhang, X. Li, G. Qi, *ChemPhysChem* **2010**, *11*, 2432-2437. (c) O. Sel, T. Azais, M. Maréchal, G. Gébel, C. Laberty-Robert, C. Sanchez, *Chem. Asian J.* **2011**, *6*, 2992 -3000. (d) C. Sanchez, B. Julián, P. Belleville, M. Popall, *J. Mater. Chem.* **2005**, *15*, 3559-3592. (e) A. Corma, H. Garcia, *Chem. Soc. Rev.* **2008**, *37*, 2096-2126. (f) J. Wang, M. Musameh, Y. Lin, *J. Am. Chem. Soc.* **2003**,*125*, 2408-2409. (g) L.A. Hirano, M.T. Escote, L.S. Martins-Filho, G.L. Mantovani, C.H. Scuracchio, *Artif. Organs* **2011**, *35*, 478-483. (h) M. Wirtz, M. Parker, Y. Kobayashi, C.R. Martin, *Chem. Eur. J.* **2002**, *8*, 3572-3578. (i) J.L. Duan, T.W. Cornelius, J. Liu, S. Karim,; H.J. Yao, O. Picht, M. Rauber, S. Müller, R. Neumann, *J. Phys. Chem. C* **2009**, *113*, 13583-13587. (j) G. Santoro, S. Yu, M. Schwartzkopf, P. Zhang, S. K. Vayalil, J. F. H. Risch, M. A. Rübhausen, M. Hernández, C. Domingo, S. V. Roth; *Appl. Phys. Lett* **2014**, 104 (24), 243107.

(3) (a) P. Liu, J. Bandara, Y. Lin, D. Elgin, L.F. Allard, Y.-P. Sun, *Langmuir* **2002**, *18*, 10389–10401. (b) N.H. Jalani, K. Dunn, R. Datta, *Electrochim. Acta* **2005**, *51*, 553-560. (c) X. Teng, Y. Zhao, J. Xi, Z. Wu, X. Qiu, L. Chen, *J. Membr. Sci.* **2009**, *341*, 149-154. (d) H.W. Rollins, F. Lin, J. Johnson, J.-J. Ma, J.-T. Liu, M.-H. Tu, D.D. DesMarteau, Y.-P. Sun, *Langmuir* **2000**, *16*, 8031-8036. (e) Y.-P. Sun, P. Atorngitjawat, Y. Lin, P. Liu, P. Pathak, J. Bandara, D. Elgin, M. Zhang, *J. Membr. Sci.* **2004**, 245, 211-217. (f) S. Wang, P. Liu, X. Wang, X. Fu, *Langmuir* **200**5, *21*, 11969-11973. (g) Q. Zhang, C.Z. Huang, J. Ling, Y.F. Li, *J. Phys. Chem. B* **2008**, *112*, 16990-16994. (h) M.P. Rodgers, Z. Shi, S. Holdcroft, *J. Membr. Sci.* **2008**, *325*, 346-356. (i) T. Hasegawa, T. Strunskus, V. Zaporotjenko, F. Faupel, M. Mizuhata, *ECS Trans.* **2012**, *41*, 9−18.

(4) (a) C. Heitner-Wirguin, *J. Membr. Sci.* **1996**, *120*, 1-33. (b) K.A. Mauritz, R.B. Moore, *Chem. Rev.* **2004**, *104*, 4535-4585.

(5) (a) W.Y. Hsu, T.D. Gierke, *J. Membr. Sci.* **1983**, *13*, 307-326. (b) W.Y. Hsu, T.D. Gierke, *Macromolecules* **1982**, *15*, 101-105. (c) E.M. Lee, R.K. Thomas, A.N. Burgess, D.J. Barnes, A.K. Soper, A.R. Rennie, *Macromolecules* **1992**, *25*, 3106−3109. (d) K. Schmidt-Rohr, Q. Chen, *Nat. Mater.* **2008**, *7*, 75−83. (e) L. Rubatat, A.L. Rollet, G. Gebel, O. Diat, *Macromolecules* **2002**, *35*, 4050-4055. (f) L. Rubatat, G. Gebel, O. Diat, *Macromolecules* **2004**, *37*, 7772−7783.

(6) J.A. Elliott, D. Wu, S.J. Paddison, R.B. Moore, *Soft Matter* **2011**, *7*, 6820-6827.

(7) (a) R. Kumar, A.K. Pandey, S. Dhara, N. L. Misra, S. V. Ramagiri, J. R. Bellare, A. Goswami, *J. Membr. Sci.* **2010**, *352*, 247-254. (b) R. Kumar, A.K. Pandey, S. Das, S. Dhara, N.L. Misra, R. Shukla, A.K. Tyagi, S.V. Ramagiri, J.R. Bellare, A. Goswami, *Chem. Commun.* **2010**, *46*, 6371-6373. (c) S. Patra, D. Sen, A. K. Pandey, C. Agarwal, S. V. Ramagiri, J. R. Bellare, S. Mazumder, A. Goswami, *J. Phys. Chem. C.* **2013**, *17*, 12026-12037. (d) S. Patra, A. K. Pandey, D. Sen, S. V. Ramagiri, J. R. Bellare, S. Mazumder, A. Goswami, *Langmuir,* 2014, **30**, 2460−2469.

(8) L. Suber, W.R. Plunkett, *Nanoscale* **2010**, *2*, 128-133

(9) A. Goswami, A. Acharya, A.K. Pandey, *J. Phys. Chem. B.* **2001**,*105*, 9196-9201.

(10) A. Sachdeva, S. Sodaye, A.K. Pandey, A. Goswami, *Anal. Chem.* **2006**, *78*, 7169-7174.

(11) (a) A. Buffet, A. Rothkirch, R. Dohrmann, V. Korstgens, M.M.A. Kashem, J. Perlich, G. Herzog, M. Schwartzkopf, R. Gehrke, P. Muller-Buschbaum, S. V. Roth, *J. Synchr. Radiation.* **2012**, *19*, 647-653. (b) G. Santoro, A. Buffet, R. Döhrmann, S. Yu, V. Körstgens, P. Müller-Buschbaum, U. Gedde, M. Hedenqvuist, S. V. Roth, *Rev. Sci. Instrum.***2014**, *85*, 043901.

(12) K. Jomova, M. Valko, *Toxicology* **2011**, *283*, 65.

(13) S. P. Mushran, M. C. Agrawal, R. M. Mehrotra, R. Sanehi, *J. Chem. Soc., Dalton Trans*., 1974, 1460-1462 DOI: 10.1039/DT9740001460.

(14) M. Krumrey, G. Gleber, F. Scholze, J. Wernecke, *Meas. Sci. Technol.* **2011**, *22*, 094032 (6pp).

(15) M. Takesue,; T. Tomura, M. Yamada, K. Hata, S. Kuwamoto, T. Yonezawa, *J. Am. Chem. Soc.* **2011**, *133*, 14164-14167.
(16) (a) C. Amano, H. Niina, Y. Mikami, *J. Mol. Struct.: THEOCHEM* **2009**, *904*, 64-68. (b) M. Harb, F. Rabilloud, D. Simon, *Phys. Chem. Chem. Phys.* **2010**, *12*, 4246-4254.
(17) (a) A. Gangula, R. Podila, M. Ramakrishna, L. Karanam, C. Janardhana, A. M. Rao, *Langmuir*, 2011, 27, 15268-15274. (b) Z.D. Pozun, S.E. Rodenbusch, E. Keller, K. Tran, W. Tang, K. J. Stevenson, G. Henkelman, *J. Phys. Chem. C*, 2013, 117, 7598−7604. (c) V. K. Vidhu, D. Philip, *Micron*, **2014**, 56, 54-62. (d) V. S. Suvith, D. Philip, *Spectrochimica Acta Part A: Molecular and Biomolecular Spectroscopy*, **2014**, 118, 526–532. (e) S. Patra, A. K. Pandey, S. K. Sarkar, A. Goswami; *RSC Advances*, **2014**, 4, 33366-33369.
(18) C. Ray, S. Dutta, S. Sarkar, R. Sahoo, A. Roy, T. Pal; *RSC Advances*, **2013**, 3, 24313-24320.